CFSRC COLLOQUIUM

Proceedings of the Cold-Formed Steel Research Consortium Colloquium
17-19 October 2022 (cfsrc.org)

Full scale static loading and fire resistance tests of LSF mezzanine systems

M. Horáček[1], M. Karmazínová[2], M. Hladík[3], Z. Poeffel[4], O. Pešek[5], I. Balázs[6]

Abstract

The subject of the article is an experimental investigation of the actual behavior of thin-walled cold-formed C profiles used in the mezzanine systems as floor beams under the effects of static load and under the effects of fire. The aim is to determine the improved design characteristics of floor beams derived from the results of experiments, which will lead to their more economical and efficient design compared to design performed based on the rules and calculation procedures specified in the relevant European standards (Eurocodes). In total 16 static loading tests were performed on a section of the floor structure in real scale using the vacuum test method, which allows apply the uniform load. The results of static loading tests are statistically evaluated and the characteristic values of bending resistances for primary beams are derived based on the Annex D of EN 1990. Generally, the number of fire resistance tests carried out in the past on full-scale sections of load-bearing thin-walled steel structures is very limited. Therefore, standard full-scale fire resistance tests were performed on light gauge steel frame floor structures of two different configurations. First configuration includes one internal (middle) doubled primary beam and two single outer primary beams, a second configuration includes only two single outer primary beams. The fire resistance tests were performed according to EN 1365-2 „Fire resistance tests for loadbearing elements - Part 2: Floors and roofs". Both tested configurations are classified based on the EN 13501-2 „Fire classification of construction products and building elements - Part 2: Classification using data from fire resistance tests, excluding ventilation services" and compared with the predicted fire resistance calculated according to EN 1993-1-2 „Eurocode 3: Design of steel structures - Part 1-2: General rules - Structural fire design".

1. Introduction

The current trend in the design of steel structures leads, due to the material savings, to the frequent use of thin-walled cold formed steel sections. The field of their use includes many types of diverse constructions. The light steel frame (LSF) mezzanine structural systems are one of the examples of use.

In practice, the design of these constructions is carried out according to valid standards. The design procedures and stated rules are based on generalized knowledge given for a wide range of profiles, their loading and types of applications. Manufacturers of thin-walled cold-formed profiles often perform their own experimental investigation of their actual properties, because they know from practical experience that the procedures set out in the standard can lead to conservative results in many cases. On the basis of experimental verification of real behavior, manufacturers can optimize the design of their structural systems and thus achieve an increase in the competitiveness of their products.

2. Structural system of LSF mezzanines

The structural system of LSF mezzanines (fig. 1) consists of a system of thin-walled primary floor beams (girders) and secondary floor beams (joists) supported by traditional (hot-rolled) steel columns.

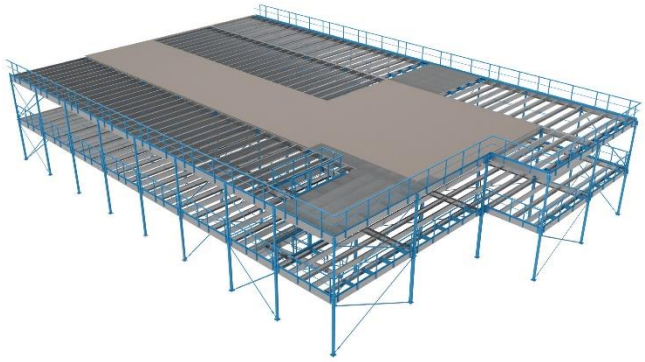

Figure 1: LSF mezzanine structural system [1]

[1] Assistant Professor, Institute of Metal and Timber Structures, Brno University of Technology – Faculty of Civil Engineering, horacek.m1@fce.vutbr.cz
[2] Professor, Institute of Metal and Timber Structures, Brno University of Technology – Faculty of Civil Engineering, karmazinova.m@fce.vutbr.cz
[3] Engineer, company director, voestalpine Profilform s.r.o., marek.hladik@voestalpine.com
[4] Engineer, voestalpine Profilform s.r.o., zbynek.poeffel@voestalpine.com
[5] Assistant Professor, Institute of Metal and Timber Structures, Brno University of Technology – Faculty of Civil Engineering, pesek.o@fce.vutbr.cz
[6] Assistant Professor, Institute of Metal and Timber Structures, Brno University of Technology – Faculty of Civil Engineering, balazs.i@fce.vutbr.cz

The columns are typically made of cold formed welded square hollow sections (tubes), complete with welded connecting plates for girders, and a base plate. The primary beams are screwed to plates welded on columns. The secondary beams are bolted to the primary beams through angle profiles. The profile depth of the primary beams and secondary beams can be identical (fig. 2) or different – profile depth of the secondary beams varies from 50% to 100% of profile depth of primary beams (fig. 3).

Figure 2: Composition of the floor structure
(identical profile depth of primary and secondary beams) [1]

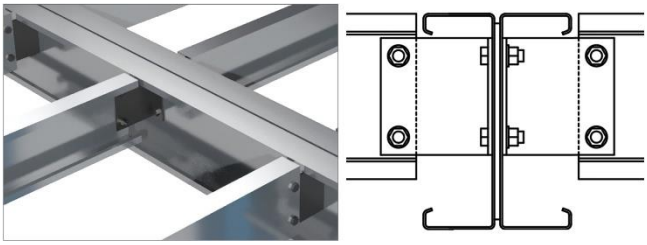

Figure 3: Detail of the floor beams connection
(different profile depth of primary and secondary beams) [1]

3. Static loading tests

Static loading tests were performed on a section of the floor structure in real scale using the vacuum test method which allows apply the uniform load (in real conditions up to 65 kN/m^2). This loading method was in Czech Republic developed by Professor Jindřich Melcher [2].

3.1 Test set up

The static loading tests were performed at Brno University of Technology, Faculty of Civil Engineering in the test laboratory of The Institute of Metal and Timber Structures. The entire test assembly is consisting of wooden box and a section of the mezzanine system, which is built into the wooden box (fig. 4). The wooden box stands on a concrete floor which is specially reinforced to be able to carry the uplift forces. The floor surface is painted in order to close pores and smaller cracks and for better adhesion of the plastic foil, which covers the entire test assembly (fig. 5). A section of the floor structure in real scale is built into the wooden box (fig. 6). The floor structure is supported by 6 short hot-rolled columns. Short primary beams are used to connect the section of the floor structure to the wooden box.

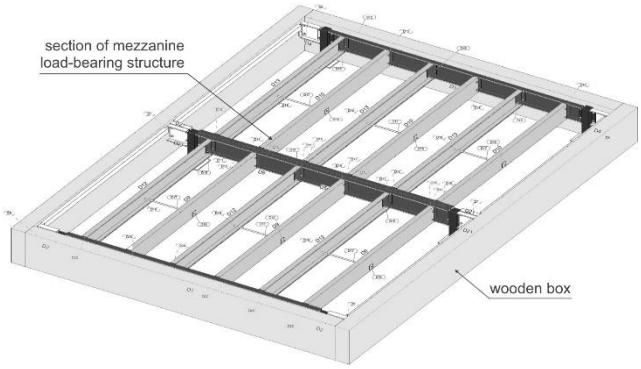

Figure 4: Test set up scheme

Figure 5: Wooden box standing on reinforced concrete floor slab

Figure 6: Test specimen installed in the wooden box

Figure 7: Test specimen with installed chipboards

All connections between primary and secondary beams are bolted via gusset plates. The floor load-bearing structure is covered by the chipboards with a thickness of 38 mm (fig. 7). The chipboard is attached to the top flanges of primary and secondary beams by means of screws (spacing of screws approx. 600 mm). The whole test assembly is covered by the plastic foil. The plastic foil is attached to the painted concrete floor with adhesive tape around the entire perimeter of the wooden box. During the testing air is extracted from the space inside the box using vacuum pump, which loads uniformly the floor structure (fig. 8).

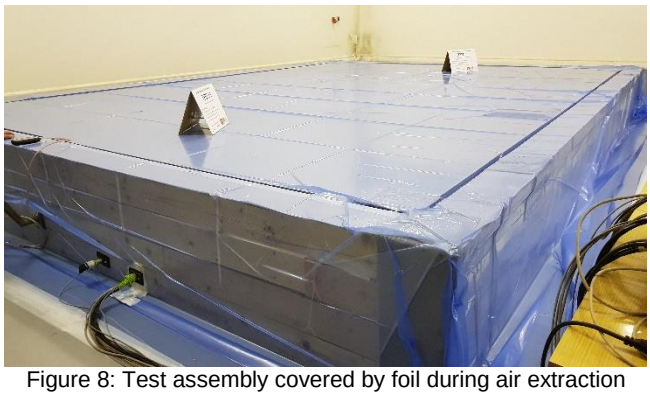

Figure 8: Test assembly covered by foil during air extraction

3.2 Description of diagnostic sensors

During the vacuum tests, the negative pressure inside the vacuum box was continuously measured by TMVG 517 Z3H sensor, range 0 – 100 kPa, Tp 0.2, manufacturer Cressto s.r.o. The stresses were measured using strain gauges (resistance strain gauges LY 11 6/350, K = 2.05, manufacturer HBM) installed on all primary floor beams (strain gauges T1 to T4) and on two selected secondary floor beams (strain gauges T5 and T6). All strain gauges were placed in the middle of the beam spans, always in the middle of the bottom flange width on the bottom surface. The layout of installed strain gauges is shown in fig. 9.

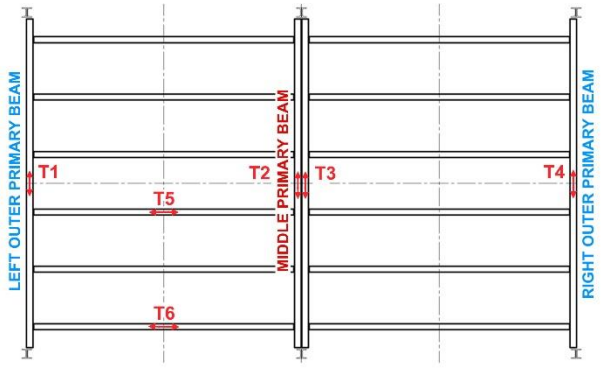

Figure 9: Position of the installed strain gauges

During the load tests, the deformations of all primary beams and one selected secondary beam were measured in the middle of their span. Two displacements were measured (fig. 10) – vertical deflection and horizontal deflection of the lower flanges (potentiometric sensors WPS-250-MK30-P10, range 0 – 250 mm, Tp 0.1, MICRO-EPSILON). For some configurations, vertical displacements were measured at the primary beams supports (inductive sensors WA50-T, range 0 - 50 mm, Tp 0.2, HBM).

Figure 10: Potentiometric sensors for measuring vertical and horizontal deflections at the beam mid-spans

3.3 Tested configurations

In total 16 static loading tests were performed. The overview of used beam profiles in tested configurations is listed in table 1. The profiles (all steel S450GD) of primary beams (PB) and secondary beams (SB) were chosen so as to verify separately the load-bearing capacity of the outer single PB and middle doubled PB, both for the case of the identical profile depths of PB and SB and for the case of different profile depths (profile depth of SB was approximately 3/4 of the profile depth of PB).

Table 1: Overview of tested configurations (beam profiles)

Test No.	Outer PS profile		Middle PB profile	SB profile
	left	right		
1	262M25	262C+25	2× 262M23	262M15
2	262M25	262C+25	2× 262M23	202M14
3	262M25	262M25	2× 262M23	262M15
4	262M25	262M25	2× 262M23	262M15
5	262C+25	262C+25	2× 262C+25	262M15
6	262M23	262M23	2× 262M23	262M15
7	262C+25	262C+25	2× 262C+25	202M18
8	262M23	262M23	2× 262M23	202M14
9	262C+25	262C+25	2× 262C+25	262M15
10	262C+25	262C+25	2× 262C+25	202M18
11	262M23	262M23	2× 262M23	262M15
12	262M23	262M23	2× 262M23	202M14
13	262C+25	262C+25	2× 262C+25	262M15
14	262C+25	262C+25	2× 262C+25	202M18
15	262M23	262M23	2× 262M23	202M14
16	262C+25	262C+25	2× 262C+25	202M18 *)

* In case of test 16 the steel grating panels were used instead of chipboards
Note: PB = primary beam; SB = secondary beam; all from steel S450GD

The following data can be determined from the profile designation: type of the cross section (M is for lipped channel section with flange edge single stiffener, C+ is for lipped channel section with flange edge double stiffener); profile depth (first number in profile designation – e.g. 262 is profile depth 262 mm); profile thickness (last number – e.g. 25 is thickness 2.5 mm).

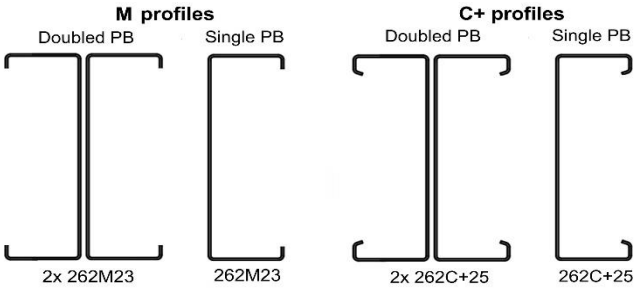

Figure 11: Tested primary beam profiles

3.4 Results of individual static loading tests

For each tested configuration, the values of the uniform load applied on the tested section of the mezzanine structure were determined when the ultimate load bearing capacity of the individual structural elements was reached. The load achived at the moment of each element failure is considered to be the element ultimate load-bearing capacity. Specifically, it is the failure of the double middle PB and two (left and right) outer single PB. In some tests, the ultimate load bearing capacity of the SB was also reached. The actual uniform loads coresponding to ultimate load-bering capacity of individual structural members is for the test No. 8 shown in fig. 12 (the load – stress diagram) and in fig. 13 (the load – deformation diagram).

When determining the load-bearing capacity of the double middle and single outer primary beams, the uniform load caused by vacuuming, the self-weight of the primary and secondary beams and chipboards are taken into account. The self-weight of the profiles of primary and secondary beams is considered according to the manufacturer's technical manual [1]. For chipboard it is calculated with a density of 650 kg/m^3.

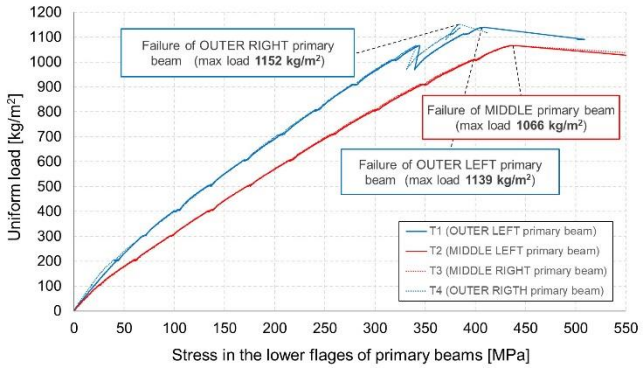

Figure 12: Load – stress diagram (test No. 8)

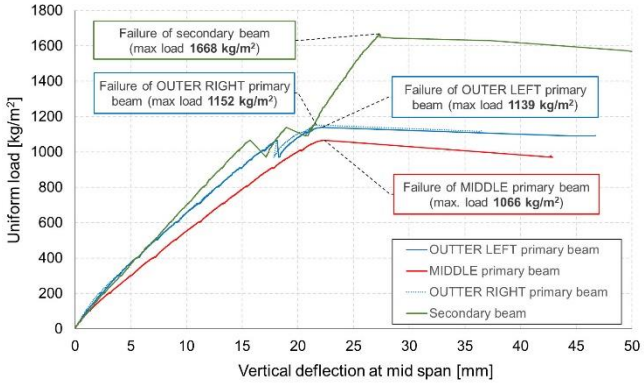

Figure 13: Load – deformation diagram (test No. 8)

For the determination of the vacuum load at the moment of primary beams failure, it is necessary to determine the share of the actual level of load transfer by the middle doubled PB and the outer single PB. In the case where the connection of the secondary beams to primary beams is considered to be fully hinged, with the identical length of secondary beams in both left and right part, the middle doubled PB would carry twice the load compared to the outer single PB (the middle PB has two times wider loading width compared to the outer PB). From the measurement results of the individual tests, it was proven that the connections of the secondary beams to the primary beams have a non-negligible rotational stiffness, which means that this connection does not behave as a purely hinged connection. The floor chipboard mainly contributes to the rotational stiffness of the connection. To determine the load transfer ratio through the middle doubled PB and outer sigle PB, the data from the measurement of outer and middle PB deflections from tests No. 5 to 15 were used (in these tests, the identical profiles were used for the middle and outer PB). The relation between the actual applied uniform load on the actual primary outer to middle beams deflection ratio is shown in fig. 14, from which the factor 1.1 is being derived.

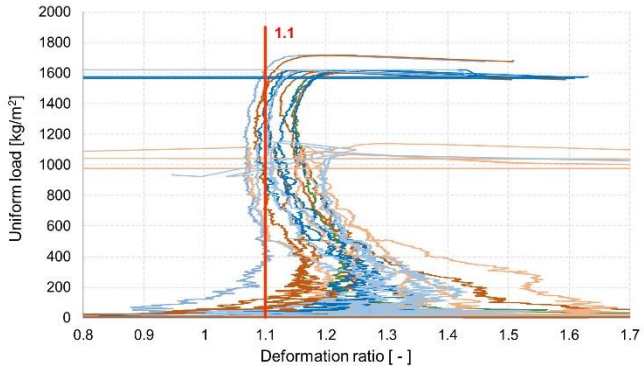

Figure 14: Outer to middle PB vertical deflection ratio

3.5 Primary beams failure mode

At the moment of the primary beams collapse (fig. 15), the local failure of the compressed flange in the middle of the

beam span in the region with the highest bending moment due to buckling was observable.

Figure 15: Collapsed load bearing structure of the mezzanine

Figure 16: Failure mode of middle double primary beam

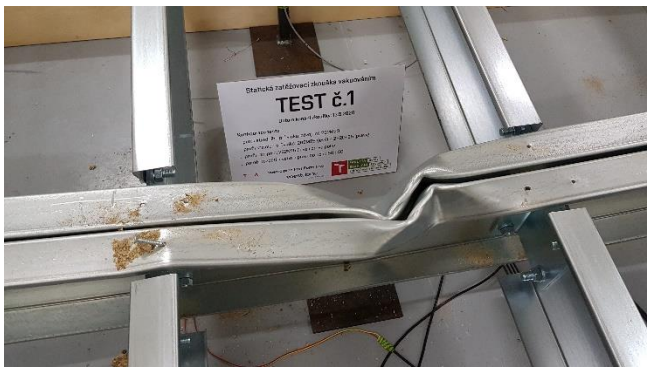

Figure 17: Progressed failure mode of middle double primary beam

Figure 18: Failure mode of outer single primary beam

The failure occurs in the section between a pair of adjacent secondary beams that stabilize the primary beams. Fig. 16 and 17 show typical failure mode of middle doubled primary beam, fig.18 shows typical failure mode for outer single primary beam.

3.6 Determination of primary beams load bearing capacity

According to Annex D of the standard EN 1990 Eurocode: Basis of structural design [3], the characteristic bending capacity of the tested profiles is determined on the basis of experimentally determined data. In general, the following relationship applies to determining the characteristic resistance based on *n* performed tests:

$$X_{\mathrm{k(n)}} = m_{\mathrm{x}} \cdot (1 - k_{\mathrm{n}} \cdot v_{\mathrm{x}}) \qquad (1)$$

where $X_{\mathrm{k(n)}}$ is resistance characteristic value (in this case bending resistance M_{Rk}),
m_{x} is the mean value of the resistances determined by individual tests,
v_{x} is the coefficient of variation,
k_{n} is the coefficient according to table 2.

Table 2: Values of k_n for a 5% characteristic value

*n**	1	2	3	4	5	6	8	10
v_x known	2.31	2.01	1.89	1.83	1.80	1.77	1.74	1.72
v_x unknown	-	-	3.37	2.63	2.33	2.18	2.00	1.92

* Original table in Annex D of EN 1990 contains k_n values also for $n > 10$

The evaluation of characteristic value (5% fractile) of bending resistance obtained from individual tests is performed within four groups of tests: M profiles for middle doubled PB, M profiles for outer single PB, C+ profiles for middle doubled PB and C+ profiles for outer single PB. The evaluation is separately done for PB and SB of identical profile depth and for PB and SB of different profile depth (SB profile depth is equal approx. to 3/4 of the PB profile depth). Table 3 summarizes the ultimate bending resistances obtained from all four groups of tests for the identical primary and secondary beam profile depth. The same resistances are listed in table 4 for all four group of tests with different primary and secondary beam profile depth. These resistances in both tables include the correction by the factor representing the ratio between the material nominal and actual yield stress of the primary beams. The coupon tests were used for the determination of the actual yield stress.

Table 3: Corrected bending resistances $M_{\mathrm{test,corr}}$ [kNm] derived from tests with identical primary and secondary beam profile depth

Primary beam profile	1	2	3	4	5
262 M 23 (middle)	28.57	28.21	29.11	28.55	27.28
262 M 23 (outer)	25.41	26.13	-	-	-
262 C+ 25 (middle)	40.24	39.90	40.16	-	-
262 C+ 25 (outer)	36.82	36.93	37.15	-	-

Table 4: Corrected bending resistances $M_{test,corr}$ [kNm] derived from tests with different primary and secondary beam profile depth

Primary beam profile	1	2	3	4	5
262 M 23 (middle)	26.84	26.74	26.51	-	-
262 M 23 (outer)	25.88	26.19	26.51	-	-
262 C+ 25 (middle)	40.39	40.29	40.39	-	-
262 C+ 25 (outer)	36.67	38.10	37.93	-	-

The evaluation of characteristic value (5% fractile) of bending resistance obtained from individual tests is performed for each group of tests in table 5 (for the case of tests with identical primary and secondary beam profile depth) and table 6 (for the case of tests with different profile depth of primary and secondary beams).

Table 5: Evaluation of characteristic value of bending resistance from test results with identical primary and secondary beam profile depth

Primary beam profile	m_x	v_x	n_{tests}	k_n	M_{Rk}
262 M 23 (middle)	28.34	0.024	5	2.33	26.77
262 M 23 (outer) *	25.77	0.020	2	-	-
262 C+ 25 (middle)	40.10	0.004	3	3.37	39.49
262 C+ 25 (outer)	36.97	0.005	3	3.37	36.40

*Insufficient number of valid test results within this group for the evaluation

Table 6: Evaluation of characteristic value of bending resistance from test results with different primary and secondary beam profile depth

Primary beam profile	m_x	v_x	n_{tests}	k_n	M_{Rk}
262 M 23 (middle)	26.70	0.006	3	3.37	26.14
262 M 23 (outer)	26.19	0.012	3	3.37	25.12
262 C+ 25 (middle)	40.35	0.001	3	3.37	40.17
262 C+ 25 (outer)	37.57	0.021	3	3.37	34.93

3.7 Results comparison with Eurocode calculations

Fig. 19 shows the comparison of experimentally verified characteristic bending resistances with the resistances calculated according to current valid European standards EN 1993-1-3 Eurocode 3: Design of steel structures - Part 1-3: General rules - Supplementary rules for cold-formed members and sheeting [4], and EN 1993-1-5 Eurocode 3: Design of steel structures - Part 1-5: General rules - Plated structural elements [5].

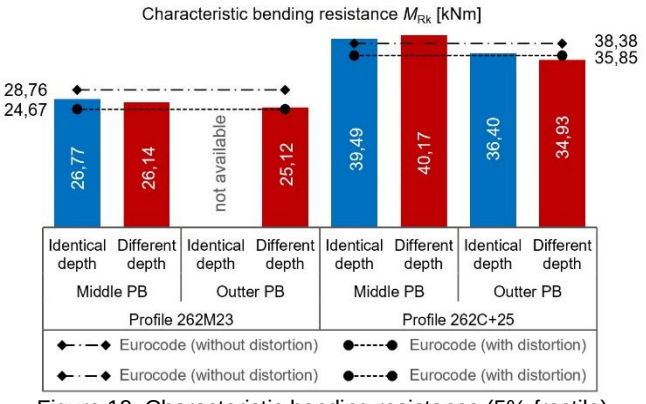

Figure 19: Characteristic bending resistance (5% fractile)

Two Eurocode characteristic resistances are plotted in fig. 19 – the characteristic bending resistance about the major axis including the effects of local buckling (in fig. 19 designated as “without distortion”) and the characteristic bending resistance about the major axis including the effects of local and distortional buckling (in fig. 19 designated as “with distortion”). This comparison shows, among other things, that the depth of the secondary beams profile in relation to the depth of the primary beams profile does not play a significant role (the differences in the characteristic bending resistances are not statistically significant). From the comparison, it can be seen that the use of beam profiles as single outer primary beams brings a reduction in load bearing capacity compared to the use of these beam profiles as doubled middle primary beams. This difference can be justified by the fact that the outer single primary beams are, unlike the middle doubled primary beams, loaded one-sided only, which causes their additional torsion.

4. Fire resistance tests

Fire tests were performed in the accredited laboratory PAVUS a.s. - Fire Testing Laboratory Veselí nad Lužnicí, Czech Republic (furnace used for testing is shown in fig. 20).


Figure 20: Test furnace fire testing laboratory

A standard full-scale fire resistance tests were performed on light gauge steel frame floor structures of two different configurations. Both tested configurations (fig. 21) include light gauge steel frame composed of cold-formed steel lipped channel primary beams and secondary beams, chipboard as floor construction and connecting angels with fasteners. First configuration includes a doubled middle primary beam (profile 2×402C+32) and two single outer primary beams (profile 402C+32), a second configuration includes only two single outer primary beams (profile 402C+32). The same secondary beams (profile C342M23) were used in both configurations. All profiles for primary and secondary beams were produced from steel grade S450GD. The span of the primary beams in both configurations was the same 5000 mm, the axial distance of the primary beams was 1653 mm in the case of configuration A, respectively 2000 mm in configuration B.

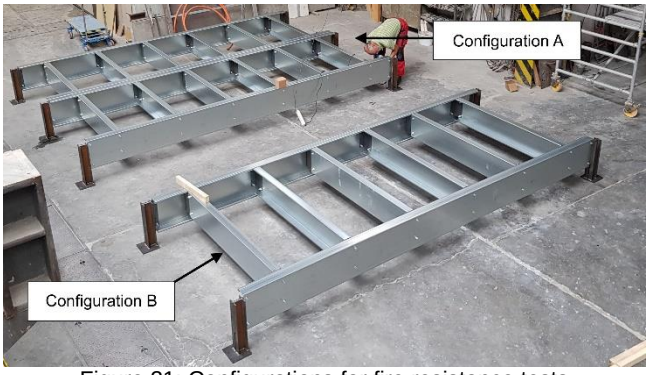

Figure 21: Configurations for fire resistance tests

The test specimens were supported by short (length 550 mm) steel hot-rolled columns. The test specimens were seated on the test furnace (fig. 22), columns were spot welded to the rigid thresholds of the test furnace. The sides of the specimen were left free for the purpose of the test, without restricting the deflection of the loaded structure. Along the entire perimeter of test specimen, the walls from white aerated concrete blocks were built in order to close the test furnace. The gaps between blocks and specimen were sealed by mineral wool strips. The view on test specimen of configuration A from the heated side (inside the furnace) is shown in fig. 23.

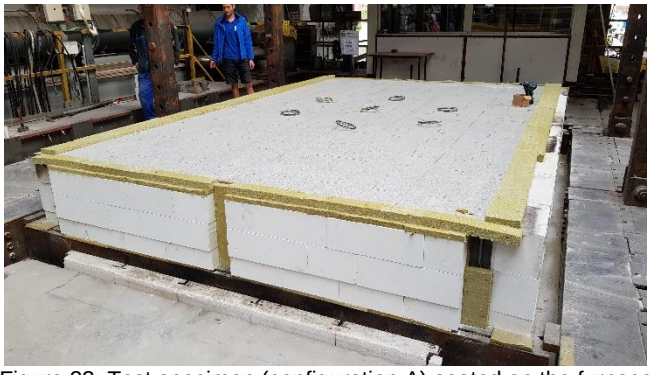
Figure 22: Test specimen (configuration A) seated on the furnace


Figure 23: Test specimen (configuration A) from heated side

The specimens were loaded from above by a system of loads (fig. 24) simulating a uniform continuous load with an intensity of 1.68 kN/m^2 (configuration A) or 1.52 kN/m^2 (configuration B). Magnitude of load was determined based on the provisions in chapter 4.2.4 of EN 1993-1-2 [6] to meet the design fire resistance R30. Loads formed by a set of steel loads were underlain by narrow strips of mineral wool in order to minimize the size of the contact area of the load with the specimens.


Figure 24: Applied load on test specimen (configuration A)

4.1 *Test procedure*

The fire resistance tests were performed according to EN 1365-2 Fire resistance tests for loadbearing elements - Part 2: Floors and roofs [7]. Test furnace was heated by a system of diesel burners. Furnace temperatures are measured by plate temperature sensors and recorded at minute intervals. The temperatures in the furnace were regulated so that within the prescribed tolerances (see [8] Article 5.1.2) they correspond to the relationship according to [8] Article 5.1.1:

$$T = 345 \cdot \log(8t + 1) + 20 \qquad (2)$$

where T is desired temperature in furnace at the time t (°C),
t is time from the start of the test (min).

4.2 *Fire resistance test results*

Both tested configurations were classified based on the EN 13501-2 „Fire classification of construction products and building elements - Part 2: Classification using data from fire resistance tests, excluding ventilation services" with fire resistance R30. The speed of the primary beams deformation was decisive. The test results are fully in line with the expected fire resistances of both configurations, which were determined according to EN 1993-1-2 „Eurocode 3: Design of steel structures - Part 1-2: General rules - Structural fire design [6]. In fig. 25 and 26 is shown the configuration A after different duration of effects of elevated temperature. Fig. 27 illustrates the whole test specimen of configuration A after the burning and extinction (photo taken second day after the testing).

Figure 25: Test specimen of configuration A after 23 minutes of fire

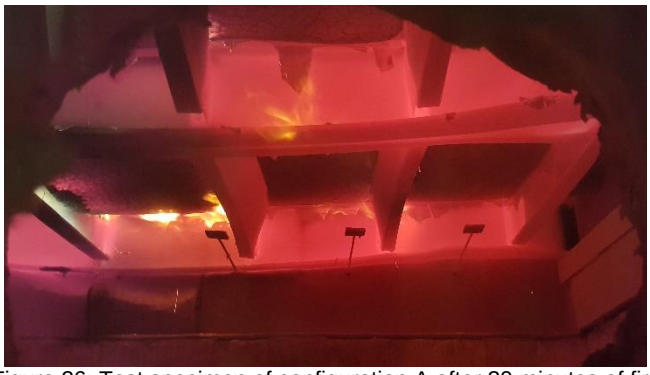

Figure 26: Test specimen of configuration A after 30 minutes of fire

Figure 27: Test specimen of config. A after burning and extinction

5. Conclusions

The performed static load tests and fire resistance tests of sections of the LSF mezzanine structure brought valuable knowledge about the real behavior of these structures.
Improved design bending resistances for some types of profiles and their specific application were derived from the static load tests. The largest increase in load bearing capacity (bending resistance about the major axis) was achieved in case of doubled middle primary beams with C+ profile. The test results of static loading tests also proved that the profile depth of the secondary beams in relation to the profile depth of the primary beam does not play a significant role in the load-bearing capacity of the primary beams. This applies to the tested profile depth ratios only (secondary beam profile depth is at least 75% of primary beam profile depth).
Although the results of fire resistance tests did not show higher fire resistance compared to calculations performed according to the relevant applicable European standards, the performed tests contributed to a better understanding of the real behavior of the entire structural system of mezzanine systems at elevated temperatures. Many examples are also known in practice where the fire protection authorities assessing a project at the stage of its approval question fire resistance calculations performed in accordance with the relevant applicable standards. Evidence of these normative calculations on the protocols for the performed fire resistance tests (including the classification of fire resistance) leads to proving the correctness of the performed calculations. The detailed information about the performed fire resistance tests are planned to be published soon in a journal paper.

6. Acknowledgments

The authors gratefully acknowledge to the Technology Agency of the Czech Republic – TACR (www.tacr.cz) for its support under the framework of research project FW01010206.

References

[1] Technical Manual: METSEC Mezzanine Floors. voestalpine Profilform s.r.o.
[2] MELCHER, J. Behaviour of thin-walled corrugated sheets and restrained beams, Proceedings of IABSE Colloquium on Thin-Walled Metal Structures in Buildings, IABSE, Stockholm, 1986, pp. 199-206.
[3] EN 1990 Eurocode: Basis of structural design. Brussels: CEN, 2002.
[4] EN 1993-1-3 Design of steel structures - Part 1-3: General rules - Supplementary rules for cold-formed members and sheeting. Brussels: CEN, 2006.
[5] EN 1993-1-5 Eurocode 3: Design of steel structures - Part 1-5: General rules - Plated structural elements. Brussels: CEN, 2006.
[6] EN 1993-1-2 Eurocode 3: Design of steel structures - Part 1-2: General rules - Structural fire design. Brussels: CEN, 2006.
[7] EN 1365-2 Fire resistance tests for loadbearing elements - Part 2: Floors and roofs. Brussels: CEN, 2014.
[8] EN 1363-1 Fire resistance tests - Part 1: General requirements. Brussels: CEN, 2020.